

# Enhanced photo-assisted electrical gating in vanadium dioxide based on saturation-induced gain modulation of erbium-doped fiber amplifier

Yong Wook Lee,<sup>1,2,\*</sup> Bong-Jun Kim,<sup>1</sup> Sungyoul Choi,<sup>1</sup> Yong Wan Lee,<sup>3</sup> and Hyun-Tak Kim<sup>1\*\*</sup>

<sup>1</sup>*Metal-Insulator Transition Project, Electronics and Telecommunications Research Institute, 161 Gajeong-dong, Yuseong-gu, Daejeon 305-350, Korea*

<sup>2</sup>*School of Electrical Engineering, Pukyong National University, San 100 Yongdang-dong, Nam-gu, Busan 608-739, Korea*

<sup>3</sup>*Department of Electrical and Computer Engineering, University of Minnesota, Minneapolis, MN 55455, USA*

\* [yongwook@pknk.ac.kr](mailto:yongwook@pknk.ac.kr), \*\* [htkim@etri.re.kr](mailto:htkim@etri.re.kr)

**Abstract:** By incorporating saturation-induced gain modulation of an erbium-doped fiber amplifier (EDFA), we have demonstrated a high-speed photo-assisted electrical gating with considerably enhanced switching characteristics in a two-terminal device fabricated by using vanadium dioxide thin film. The gating operation was performed by illuminating the output light of the EDFA, whose transient gain was modulated by adjusting the chopping frequency of the input light down to 1 kHz, onto the device. In the proposed gating scheme, gated signals with a temporal duration of ~40  $\mu$ s were successively generated at a repetition rate of 1 kHz.

©2009 Optical Society of America

**OCIS codes:** (160.6990) Transition-metal-doped materials; (140.3440) Laser-induced breakdown; (060.2410) Fibers, erbium; (230.4480) Optical amplifiers.

---

## References and links

1. M. A. Richardson, and J. A. Coath, "Infrared optical modulators for missile testing," *Opt. Laser Technol.* **30**(2), 137–140 (1998).
2. S. Chen, H. Ma, X. Yi, H. Wang, X. Tao, M. Chen, X. Li, and C. Ke, "Optical switch based on vanadium dioxide thin films," *Infrared Phys. Technol.* **45**(4), 239–242 (2004).
3. F. J. Morin, "Oxides which show a metal-to-insulator transition at the neel temperature," *Phys. Rev. Lett.* **3**(1), 34–36 (1959).
4. E. Arcangeletti, L. Baldassarre, D. Di Castro, S. Lupi, L. Malavasi, C. Marini, A. Perucchi, and P. Postorino, "Evidence of a pressure-induced metallization process in monoclinic VO<sub>2</sub>," *Phys. Rev. Lett.* **98**, 196406(1–4) (2007).
5. Y. W. Lee, B.-J. Kim, S. Choi, H.-T. Kim, and G. Kim, "Photo-assisted electrical gating in a two-terminal device based on vanadium dioxide thin film," *Opt. Express* **15**(19), 12108–12113 (2007), <http://www.opticsexpress.org/abstract.cfm?URI=oe-15-19-12108>.
6. A. Cavalleri, Cs. Tóth, C.W. Siders, J. A. Squier, F. Ráksi, P. Forget, and J. C. Kieffer, "Femtosecond structural dynamics in VO<sub>2</sub> during an ultrafast solid-solid phase transition," *Phys. Rev. Lett.* **87**, 237401(1–4) (2001).
7. H.-T. Kim, B.-G. Chae, D.-H. Youn, S.-L. Maeng, G. Kim, K.-Y. Kang, and Y.-S. Lim, "Mechanism and observation of Mott transition in VO<sub>2</sub>-based two- and three-terminal devices," *N. J. Phys.* **6**, 52–70 (2004).
8. W.-S. Choi, N.-J. Park, D.-Y. Lee, and D.-S. Hyun, "A new control scheme for a class-d inverter with induction heating jar application by constant switching frequency," *J. Power Electron.* **5**, 272–281 (2005).
9. B. K. Ridley, and T. B. Watkins, "The possibility of negative resistance effects in semiconductors," *Proc. Phys. Soc. Lond.* **78**(2), 293–304 (1961).
10. N.-S. Lee, J.-S. Chang, and Y.-S. Kwon, "Determination of the NDR and electron transport properties of self-assembled nitro-benzene monolayers using UHV-STM," *KIEE J. Electr. Eng. Technol.* **1**, 366–370 (2006).
11. D. Silber, W. Winter, and M. Fullmann, "Progress in light activated power thyristors," *IEEE Trans. Electron. Dev.* **23**(8), 899–904 (1976).
12. R. F. Carson, R. C. Hughes, T. E. Zipperian, H. T. Weaver, T. M. Brennan, B. E. Hammons, and J. F. Klem, "High-voltage, wavelength-discriminating, light-activated GaAs thyristor," *Electron. Lett.* **25**(23), 1592–1593 (1989).
13. C.-K. Kim, B.-M. Yang, and H.-S. Lee, "A dynamic performance study of an HVDC system using a hybrid simulator," *J. Power Electron.* **5**, 319–328 (2005).
14. Y.-W. Choi, and J. Kim, "Sputtering technique of magnetism oxide thin film for plasma display panel applications," *KIEE J. Electr. Eng. Technol.* **1**, 110–113 (2006).

15. D. J. Hilton, R. P. Prasankumar, S. Fourmaux, A. Cavalleri, D. Brassard, M. A. El Khakani, J. C. Kieffer, A. J. Taylor, and R. D. Averitt, "Enhanced photosusceptibility near  $T_c$  for the light-induced insulator-to-metal phase transition in vanadium dioxide," *Phys. Rev. Lett.* **99**, 226401(1–4) (2007).
  16. C. R. Giles, E. Desurvire, and J. R. Simpson, "Transient gain and cross talk in erbium-doped fiber amplifiers," *Opt. Lett.* **14**(16), 880–882 (1989).
  17. E. Desurvire, "Analysis of transient gain saturation and recovery in erbium-doped fiber amplifiers," *IEEE Photon. Technol. Lett.* **1**(8), 196–199 (1989).
- 

## 1. Introduction

Up to the present, it has been found that a phase transition (PT) between insulating and metallic states in vanadium dioxide ( $\text{VO}_2$ ) thin film, intensively being studied due to its potential in high-speed optical devices [1,2], could be induced by temperature [3], pressure [4], light [5,6], electric field [7] and so forth. In an electrical response, two-terminal electrical devices based on  $\text{VO}_2$  thin films ( $\text{VO}_2$  device) show strong nonlinear current-voltage ( $I$ - $V$ ) behaviors [7]; in other words, an abrupt current jump takes place at a specific threshold voltage ( $V_T$ ), and this current jump can be usefully applied to electrical switching devices like thyristors [8] based on negative differential resistance characteristics [9,10]. Recently, it was reported that  $V_T$  of the  $\text{VO}_2$  device could be controlled by the intensity adjustment of the light directly illuminated onto the  $\text{VO}_2$  film of the device, i.e., the photo-assisted electrical gating in the  $\text{VO}_2$  device was embodied [5]. The optical gating scheme can be directly applied to the light triggered thyristors [11,12] recently being adopted for many power stations, substations, and power utilities for trains and automobiles [13]. In the previous study [5], however, the optical switch, whose switching speed was  $\sim 1$  ms, was employed for the modulation of the cw input light, and the temporal duration of the optical switching pulse for the optical gating could not be reduced to  $< 2$  ms due to the limit of the switching speed of the optical switch. In this paper, we have demonstrated a high-speed photo-assisted electrical gating in the  $\text{VO}_2$  devices by incorporating the saturation-induced gain modulation (SIGM) of an erbium-doped fiber amplifier (EDFA), which was used only for the amplification of the illumination light in [5], without an additional high-speed optical modulator. For the implementation of the high-speed optical gating, a transient gain of the EDFA was modulated by adjusting the chopping frequency of the input light down to 1 kHz, and overshoot-like short optical pulse peaks could be generated in the amplifier output by the gain modulation. In the proposed gating system, gated signals with a temporal duration of  $\sim 40$   $\mu\text{s}$ , which was reduced by  $> 50$  times compared with that obtained in [5], were successively generated at a repetition rate of 1 kHz.

## 2. Experimental setups

Figure 1 shows the schematic diagram of the experimental setup, composed of the infrared light illumination and the electrical measurement sections, for implementing the high-speed optical gating in the fabricated  $\text{VO}_2$  devices. The cross-section and plane-view of the  $\text{VO}_2$  device are also shown. In the optical part, a 1550 nm laser output of a distributed feedback laser diode (LD) goes into an optical chopper (OC) equipped with a U-shaped bracket, and the modulated light from the OC enters an EDFA (Luxpert) to amplify its intensity. The OC (Thorlabs MC2000) has a chopping frequency from 1 Hz to 6 kHz and a frequency drift  $< 20$  ppm/ $^\circ\text{C}$ . The bracket with a single-mode fiber pigtail at each end has a 0.51" air gap and an insertion loss  $< 2.5$  dB. Through a 50:50 fiber coupler, the amplified output from the EDFA is separated into two light components. One component is introduced into the fiber-pigtailed focuser for conveying the light to the  $\text{VO}_2$  film, and the other component into an optical spectrum analyzer (Yokogawa AQ6370) for monitoring its output spectrum. The output beam from the fiber focuser is launched into the film at  $30^\circ$  incidence. The location of the focuser, whose spot diameter at beam waist and working distance to beam waist were designed as  $\sim 18$   $\mu\text{m}$  and  $\sim 10$  mm, respectively, was precisely adjusted for the beam spot diameter to be  $\sim 300$   $\mu\text{m}$  using an  $xyz$  translation stage. For electrical measurements using a parameter analyzer (HP 4156C), the micromanipulator was employed for the minute position control of the metal tip brought into contact with the electrodes of the  $\text{VO}_2$  devices. The  $\text{VO}_2$  films (thickness:  $\sim 100$  nm) and devices were prepared by the same fabrication processes as those adopted in

[5]. One different part in the devices was Ni/Au electrodes formed by the sputtering technique [14]. In order to obtain the samples with optimal performance, a few hundreds of VO<sub>2</sub> devices with various dimensions (L × W), where L and W were the electrode interval and the film width, respectively, were fabricated, and the device with the dimension of 5 × 20 μm<sup>2</sup> was selected for the experiment.

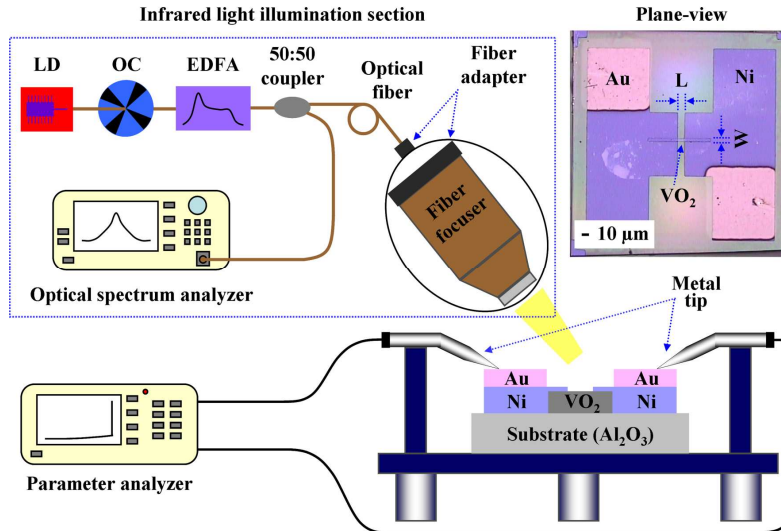


Fig. 1. Experimental setup for high-speed photo-assisted electrical gating.

### 3. Experimental results and discussions

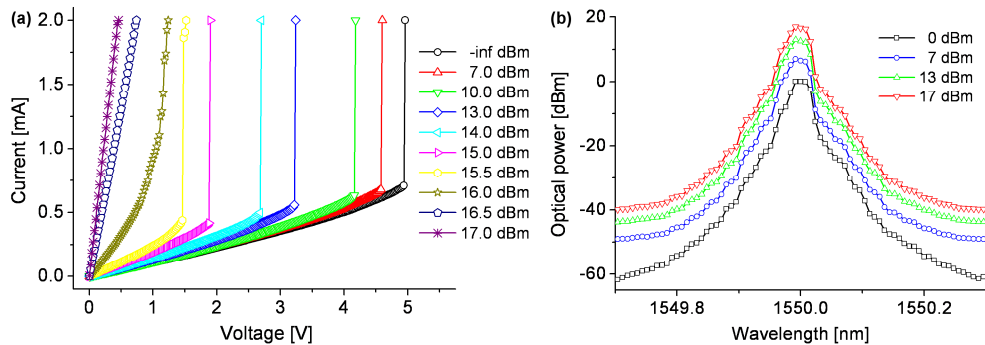


Fig. 2. (a) *I-V* properties of the VO<sub>2</sub> device when the infrared light with various intensities is illuminated and (b) optical spectra of the illumination light at various intensities.

Figure 2(a) shows *I-V* characteristics of the fabricated VO<sub>2</sub> device in a voltage-controlled mode when an infrared light with various intensities, which is provided by amplifying the LD output through the EDFA, is illuminated onto the device without the OC. For preventing high current flow, the electrical current flowing through the device was limited to 2 mA. Without illumination (-inf dBm), an abrupt current jump is observed at a specific  $V_T$  of ~5.0 V. As the light intensity increases,  $V_T$  decreases and moves toward 0 V. At the light intensity of 16.0 dBm, some peculiar phenomenon is observed that the abrupt current jump gradually disappears. This percolative singularity that happens between both intensities of 15.5 and 16.5 dBm results from the inhomogeneity that the metallic phase (low resistance state of ~a few Ω) changed from the insulating phase (high resistance state of ~a few kΩ) due to the photo-induced PT coexists with the insulating one within the same film [15]. At more than 16.5 dBm, the metallic phase seems to dominate in the film compared with the insulating one,

and the device conductivity continuously increases with the light intensity. Until the metallic phase dominates in the film due to strong illumination  $> 15.5$  dBm,  $V_T$  can be fully tuned, and the tuning displacement can reach  $\sim 3.5$  V with respect to the optical intensity variation of 15.5 dBm ( $\sim 35.5$  mW) resulting in a tuning sensitivity of  $\sim 98.6$  V/W. Figure 2(b) shows the optical spectra of the illumination light at various intensities (0  $\sim$  17 dBm), measured by the optical spectrum analyzer with the resolution bandwidth of 0.05 nm. The center wavelength and signal to amplified spontaneous emission ratio of the illumination light were measured as  $\sim 1550$  nm and  $> 50$  dB, respectively. The optical density of the light beam projected onto the film was  $\sim 14.1$  W/cm<sup>2</sup> at the input intensity of 10 mW.

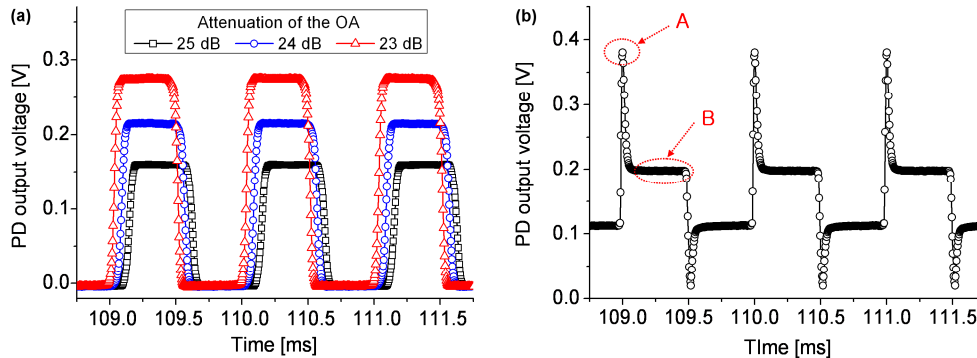


Fig. 3. (a) Photodetector output of the infrared light whose intensity is modulated at 1 kHz using an external OC and (b) transient variation of the light intensity of the EDFA output when the light signal whose intensity is modulated at 1 kHz is amplified by the EDFA.

Before we describe the implementation of a high-speed optical gating, let us investigate the SIGM of the EDFA that can be obtained when the LD output modulated by an external OC enters the EDFA. For clear comparison, the modulated light signal that is not affected by the gain modulation of the amplifier is considered first. Figure 3(a) shows the photodetector (PD) response of the LD output light whose intensity is modulated at 1 kHz through the external OC when the output intensity of the LD is 0 dBm. In order to keep the input threshold of the PD, an optical attenuator (OA) was utilized in front of the PD. The attenuation values of the OA were 23, 24, and 25 dB, and the insertion losses of the OC and OA were  $\sim 2.5$  and  $\sim 1.5$  dB, respectively. As shown in the figure, a square-shaped voltage waveform switching between a ground voltage and a peak voltage was generated at 1 kHz. At 25, 24, and 23 dB attenuation of the OA, peak voltages of  $\sim 0.160$ ,  $\sim 0.215$ , and  $\sim 0.274$  V were obtained in the PD output, respectively. Based on the measurement results, the conversion gain of the PD was calculated as  $\sim 1.442 \times 10^5$  V/W at 1550 nm. Figure 3(b) shows the transient variation of the amplified light intensity when the modulated light shown in Fig. 3(a) is amplified by the EDFA. The output intensity of the LD was also fixed as 0 dBm at 1550 nm, and the attenuation of the OA was 43 dB. The amplifier output was set as  $\sim 15.4$  dBm at 0 dBm input. As observed from the figure, the leading and trailing edges of the output pulses exhibit sharp overshoots, and these overshoots result from the SIGM of the EDFA that is an effect of the reduction in population inversion or carrier density in the amplifier [16,17].

The generation of these overshoots can be understood from the gain characteristics that the saturated gain of the amplifier is reduced with the increase of the input signal power. The leading edge of the optical pulse with a peak intensity of 0 dBm initially undergoes the unsaturated high gain of the EDFA, and then the amplifier gain decreases toward the saturated low gain with a specific time constant due to the gain saturation. At the pulse trailing edge, the saturated gain gradually recovers the initial unsaturated gain because the input intensity becomes very small. This gain dynamics of the EDFA is mediated by a time constant  $>$  tens of  $\mu$ s and is generally useful for suppressing the crosstalk caused by high-frequency variations in the population inversion of the EDFA at high bit rates  $>$  1 Gb/s. From the viewpoint of a pulse compression, however, the overshoots with short temporal durations

in the output pulses can be usefully applied to the high-speed optical gating. In these overshoots shown in Fig. 3(b), the temporal width at the saturated power level ( $\sim 0.2$  V) and the rising time were measured as  $< 70$   $\mu$ s and 20  $\mu$ s, respectively. By using the conversion gain obtained in Fig. 3(a), the optical powers conveyed to the device are estimated as  $\sim 17.2$  and  $\sim 14.4$  dBm at the peak and the saturated region of the pulse (indicated as A and B), respectively, resulting in the gain modulation of 2.8 dB at the chopping frequency of 1 kHz.

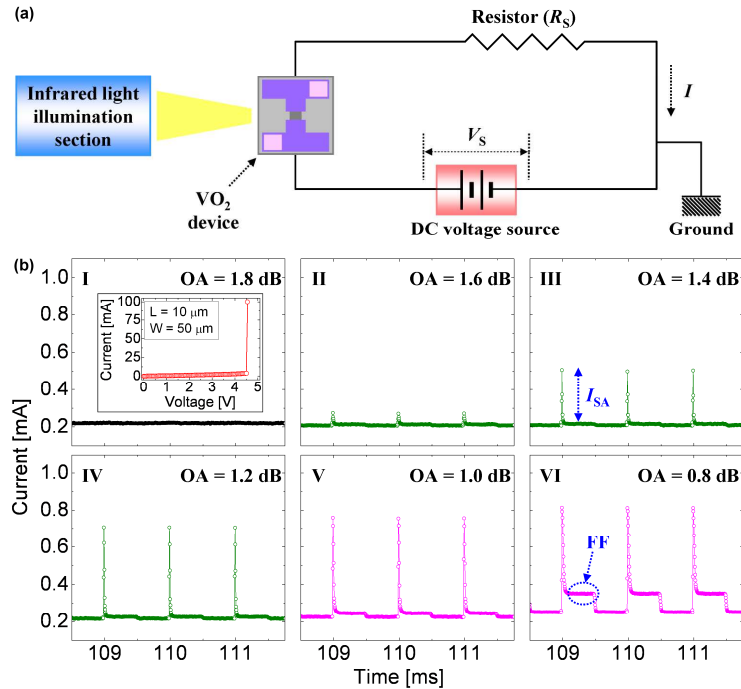


Fig. 4. (a) Electrical circuit for generating gated signals with short temporal duration based on the SIGM of the EDFA. (b) High-speed optical gating operation in the VO<sub>2</sub> device when the amplified output of the infrared light modulated at 1 kHz by the OC is shed on the VO<sub>2</sub> film with various attenuation values of the OA. Inset shows the I-V property of the VO<sub>2</sub> device (dimension:  $10 \times 50$   $\mu$ m<sup>2</sup>) measured with the compliance current of 100 mA.

In order to implement the high-speed optical gating in the VO<sub>2</sub> devices, an electrical circuit shown in Fig. 4 (a) was constructed by using a standard resistor ( $R_S$ ) connected in series with the VO<sub>2</sub> device and a DC voltage source ( $V_S$ ). The configuration of the infrared light illumination section is the same as that of the blue dotted box in Fig. 1. When  $V_S$  is set as  $< V_T$ , the device remains in its high resistance state. If  $V_T$  goes below  $V_S$  due to the illumination of the infrared light [5], however, it changes into its low resistance state. Figure 4(b) shows the transient electrical responses of the current flowing through the device ( $I$ ) when an amplified output of the infrared light modulated at 1 kHz by the OC is shed on the VO<sub>2</sub> film with  $V_S$  and  $R_S$  fixed as 1.5 V and 1.5 k $\Omega$ , respectively. The output intensity of the LD was maintained as 0 dBm at 1550 nm, and the EDFA was arranged for resulting output intensity to be  $\sim 17.4$  dBm. The attenuation of the OA was adjusted within 2 dB for varying the intensity of the light shone on the VO<sub>2</sub> device. At the attenuation value of 1.8 dB in the OA, as shown in plot I of Fig. 4(b), the gating operation does not seem to be initiated yet, and the current  $I$  flows at a shallow level designated as the dark current level ( $I_D$ ), determined by  $R_S$  and the device resistance before the transition ( $R_M \gg R_S$ ). At a fixed  $V_S$ ,  $R_M$  and thereby  $I_D$  depend mainly on the intensity of the illumination light. When the attenuation decreases to 1.6 dB (plot II), the gating operation starts, and the gated current signals whose temporal contents are  $< 40$   $\mu$ s emerge with signal amplitude (indicated as  $I_{SA}$  in plot III) of  $\sim 0.10$  mA. At the attenuation values of 1.4 and 1.2 dB, the gated current signals with temporal widths

comparable to those in plot II are observed in plots III and IV with  $I_{SA}$  of  $\sim 0.30$  and  $\sim 0.50$  mA, respectively ( $I_D = \sim 0.21$  mA). At the attenuation  $< 1.0$  dB (plots V and VI),  $I_{SA}$  of the gated signal is nearly saturated to  $\sim 0.55$  mA, and the following floor signals indicated as FF, which are unwanted signals broadening the entire pulse width of the gated signals, grow from  $I_D$  ( $\sim 0.22$  and  $0.25$  mA, respectively). These unwanted signals abruptly increase to  $\sim 0.35$  mA at the attenuation of  $0.8$  dB due to the transition of the device.

If we consider the transient intensity variation of the illumination light due to the SIGM shown in Fig. 3(b), the intensity of the light illuminated onto the device at the attenuation of  $1.0$  dB can be estimated as  $\sim 18.2$  and  $\sim 15.4$  dBm at the peak and the saturated region of the optical pulse corresponding to the gated signal and the FF signal, respectively. Similarly, in other subplots of Fig. 4(b), these light intensities carried to the device can be also obtained by associating them with the attenuation values specified in each plot, e.g., at the attenuation of  $0.8$  dB,  $\sim 18.4$  and  $\sim 15.6$  dBm at regions of the gated and the FF signals, respectively. From this intensity information, it is concluded that the transition of the device is triggered at regions of the gated and the FF signals at  $> 17.5$  and  $15.5$  dBm, respectively. From  $I$ - $V$  characteristics obtained with cw infrared light in Fig. 2(a), the device transition in the region of the FF signals at  $> 15.5$  dBm is intuitively anticipated because  $V_S$  is set as  $1.5$  V and  $V_T$  becomes  $< 1.5$  V over  $15.5$  dBm. Additional power of  $2$  dB necessary for triggering the transition in the region of the gated signals is attributed to relatively short temporal duration compared with that of the FF signals, resulting in an insufficient photo-induced excitation. In each subplot, the rising time of the gated signal was measured as  $< 10$   $\mu$ s, which was shorter than that of the illuminating optical pulses ( $\sim 20$   $\mu$ s) because the gated signal was generated over the threshold optical intensity triggering the transition. The falling time was dependent on the attenuation value of the OA, i.e., the light intensity transferred to the device and was  $2$  or  $3$  times longer than the rising one, which could be affected by the light-induced heat. Compared with the switching speed including the rising and falling times in [5], that of the proposed scheme is much faster by  $> 50$  times. In addition to the switching time of the optical pulse, the gating speed is restricted by a RC time constant ( $\sim 0.15$   $\mu$ s) of the circuit in Fig. 4(a), which can limit the maximum gating speed. In particular, the temporal width of the gated signal was independent of the chopping frequency, implying that the repetition rate can be increased up to the maximum chopping frequency to embody the SIGM. Moreover, electrical current as high as  $100$  mA can flow through the VO<sub>2</sub> channel of the junction device with the dimension adjustment ( $10 \times 50$   $\mu$ m<sup>2</sup>), as shown in inset of Fig. 4(b).

#### 4. Conclusion

In conclusion, we have investigated the enhanced photo-assisted electrical gating operation in the VO<sub>2</sub> devices by incorporating the SIGM of the EDFA. The transient gain of the amplifier was modulated by adjusting the chopping frequency of the input light down to  $1$  kHz. In the proposed gating system, the gated signals with the temporal duration of  $\sim 40$   $\mu$ s were successively generated at a repetition rate of  $1$  kHz.

#### Acknowledgments

The present research was financially supported by the "High Risk High Return Project" of ETRI and the "project on current jump" in MKE.